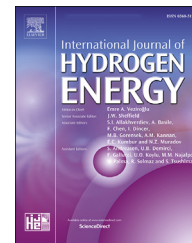




ELSEVIER

Available online at www.sciencedirect.com

ScienceDirect

journal homepage: www.elsevier.com/locate/he

Model-based degradation prediction on impedance data and artificial neural network for high-temperature polymer electrolyte membrane fuel cells after hydrogen starvation

Khrystyna Yezerska ^{a,b,*}, Anastasia Dushina ^c, Andriy Sarabakha ^d, Peter Wagner ^c, Alexander Dyck ^b, Michael Wark ^a

^a Institute of Chemistry, Carl von Ossietzky University, 26129 Oldenburg, Germany

^b DLR Institute of Networked Energy Systems, 26129 Oldenburg, Germany

^c DLR Institute of Engineering Thermodynamics, 26129 Oldenburg, Germany

^d Munich School of Robotics and Machine Intelligence (MSRM), Technical University of Munich, 80797 Munich, Germany

HIGHLIGHTS

- Artificial neural network used to predict effect of H₂ starvation of a fuel cell.
- Artificial neural network trained with long-term electrochemical data.
- First application: simulation of different long-term voltage decreases.
- Second application: fuel cell virtually kept constant after H₂ starvation.
- Results showed safe operational voltage between 0.6 and 0.51 V for stable cycling.

ARTICLE INFO

Article history:

Received 21 February 2022

Received in revised form

20 June 2022

Accepted 26 June 2022

Available online 18 August 2022

Keywords:

ANN

HT-PEM FC

H₂ starvation

Regeneration

EIS

DRT

ABSTRACT

Degradation caused by H₂ starvation is a typical reason for a limited lifetime in high-temperature polymer electrolyte membrane fuel cells (HT-PEM FC). Here, a long short-term memory (LSTM) artificial neural network (ANN), trained on experimental electrochemical data from a long-term H₂ starvation/regeneration routine, was used to predict the effect of H₂ starvation.

In a first application, different voltage decreases were simulated, which FCs typically exhibit during starvation/regeneration routines. The results of three simulation scenarios (3, 5 and 10 mV decrease per regeneration step) showed that critical resistances appeared at output voltages of 0.51, 0.49 and 0.48 V, respectively (compared to the reference voltage of 0.6 V).

In a second application, the same FC was virtually set to continue to operate normally (i.e., under regeneration conditions) at certain degrees of starvation, after which voltage was virtually kept constant at 0.48, 0.50 and 0.51 V. For 0.48 and 0.50 V, all simulated resistances fluctuated critically, which corresponded well to experimental data. However, for 0.51 V all simulated resistances never reached critical values. Hence, a safe operational

* Corresponding author. Institute of Chemistry, Carl von Ossietzky University, 26129, Oldenburg, Germany.

E-mail address: khrystyna.yezerska@uni-oldenburg.de (K. Yezerska).

<https://doi.org/10.1016/j.ijhydene.2022.06.254>

0360-3199/© 2022 Hydrogen Energy Publications LLC. Published by Elsevier Ltd. All rights reserved.

voltage range between 0.6 and 0.51 V is suggested for stable continued FC cycling, which would prevent the occurrence of more severe (irreversible) degradation.

© 2022 Hydrogen Energy Publications LLC. Published by Elsevier Ltd. All rights reserved.

Introduction

High-temperature polymer electrolyte membrane fuel cells (HT-PEM FCs) operate at ca. 160 °C [1], which offers many benefits. These are improved cathode kinetics, which include effects of temperature on reference potential, open-circuit voltage, the Tafel slope [2,3], exchange current density, oxygen transport and improved catalyst tolerance to CO [4–6] as well as improved water management and gas transport [7,8]. The performance of HT-PEM FCs has been widely studied, and a general overview of the technology is given in Ref. [9]. The key performance of each power source device is its lifetime (e.g., durability). Therefore, to extend and predict the lifetime of the HT-PEM FC, various degradation phenomena must be studied in detail, while lifetime predictions should be based on reliable modelling.

Background information on electrochemical characterization of FCs

A simple way to describe FC behaviour is given by its output voltage evolution. The basic output voltage V_{cell} produced by a single FC [10,11] is as follows:

$$V_{\text{cell}} = E_{\text{Nernst}} - V_{\text{act}} - V_{\text{ohmic}} - V_{\text{con}} \quad (1)$$

whereas E_{Nernst} is the thermodynamic potential, V_{act} is the activation voltage, V_{ohmic} is the ohmic voltage and the V_{con} is the concentration voltage.

One of the typical lifetime limitations of an HT-PEM FC is H_2 starvation (fuel undersupply). Degradation mechanisms due to H_2 starvation are described in detail in Ref. [12]. The HT-PEM FC lifetime prediction due to the H_2 starvation may be based on the voltage response after various kinds of starvation/regeneration routines. For example, Zhou et al. [8] applied an accelerated degradation test with 19 starvation steps, where the anode H_2 stoichiometry was cycled between 3.0 and 0.8 during starvation every 2 min (at constant cathode stoichiometry of 3.0). The stoichiometry factor is based on the ratio between the available gas at the inlet and the required gas necessary for the reaction. The voltage decreased from typically 0.6 V to ca. 0.2 V, which translates to a decrease by ca. 11 mV after each starvation step. A less intense voltage decrease was observed by Yezerska et al. [12], who cycled the H_2 stoichiometry between 1.5 and 1.0 (starvation) every 20 min, at a constant cathode stoichiometry of 9.5. After 55 starvation steps voltage decreased from initially 0.6 V–0.14 V, which translates to a decrease of only 1 mV for each starvation step. Hence, the lower voltage decrease may have likely been due to fewer variations in H_2 stoichiometries as well as longer regeneration time.

Fuel cell durability limitations may be described with significant deviations in externally measured currents or externally measured resistances. The latter can be determined using electrochemical impedance spectroscopy (EIS) which is a non-destructive in-situ technique [13]. Compared to other electrochemical methods, EIS offers the possibility to separate between different FC part outputs (e.g., anode and/or cathode) yielding detailed information on both, causes and locations of degradation.

The experimental results for this paper were taken from literature [12,14] in which degradation phenomena occurred during 122 starvation/regeneration steps. Hence, the empirical voltage, current and resistance data are here used to model and predict FC operation under H_2 starvation using ANN, which as the dynamic modelling tool is important for analysis, simulation, monitoring, and system control. To the best of our knowledge, this is the first work in the literature in which ANN is used to model the behaviour of HT-PEM FCs subjected to starvation/regeneration routines.

Basics on artificial neural networks and modelling approaches of FCs

Nowadays ANNs represent an important and constantly expanding field within artificial intelligence (AI) [15]. The underlying mathematical models are inspired by the functioning of biological neural networks and consist of a set of simple processing units, called neurons, which are interconnected by links, called synapses.

Hence, ANN learns from the training samples by adjusting the synaptic weights of the connections between neurons [16]. Any ANNs may be classified according to different criteria such as (i) topology: single or multilayer, (ii) type of learning: supervised or unsupervised, and (iii) type of connection between layers: feed-forward or feedback [17]. In a general single-hidden-layer ANN, the neurons are organized in (i) input layer, which receives the data, (ii) hidden layer, which embeds the knowledge of ANN, and (iii) output layer, which returns the ANN's result. Usually, ANNs reduce the need for feature engineering which is one of the most time-consuming tasks in machine learning for data training [18]. Therefore, ANNs are ideal for situations that require approximating a function that depends on inputs which nonlinearly connects to the output [19] (Fig. 1) [20,21].

The optimum number of neurons in the hidden layer is unknown and depends on the amount of empirical data. The number of neurons in the hidden layer significantly influences the capability of the network to generalize from training data [22]. A small amount of neurons lead to poor network training (underfitting) while a high amount of neurons leads to over-training (overfitting) [23].

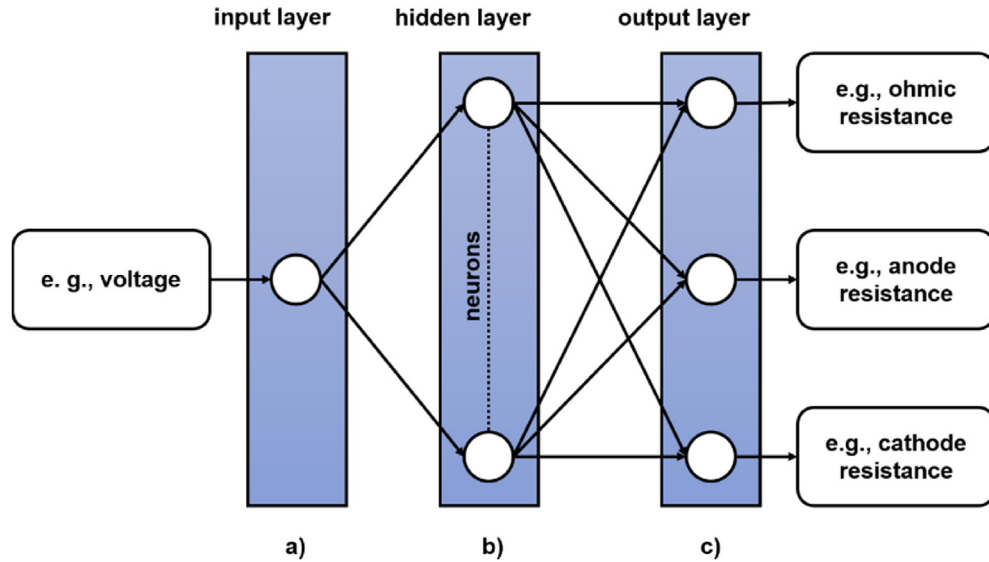


Fig. 1 – Structure of the proposed ANN architecture, with a) input layer, b) hidden layer and c) output layer.

FC modelling is typically based on numerous complex physicochemical equations and the task of ANN is to learn this complex model [20,21,24,25]. For example, Akkaya et al. [24] developed a solid oxide FC model based on an ANN approach for the FC performance prediction. Laribi et al. [25] defined a method to assess the impacts of relative humidity and operating time-based on EIS data while Shao et al. [20] and Mohammadi et al. [21] presented a fault diagnosis method for FC. Xie et al. [26] proposed a prognostic method, which allows useful life estimation and short-term degradation prediction. Recently, Gu et al. [27] proposed flooding fault diagnosis of FC using LSTM networks. Such a method has better performance in diagnose/pre-diagnose of FC.

Different operation conditions and the complexity of the FC impede the calculation of a precise voltage decrease under H_2 starvation. Therefore, FC modelling remains challenging. In this study, to train and fit ANN, we used the empirical data from Yezerska et al.'s [12] long-term FC starvation experiment such as resistance values calculated from EIS spectra, output voltage, current as well as time. First, three scenarios according to the intensity of any given starvation procedure were developed, which are reflected by different voltage decreases according to those cited above. The goal was to predict when resistances become critically high so that any FC cannot continue to run stable. Second, for the FC used in Ref. [12] three scenarios were simulated after the starvation was

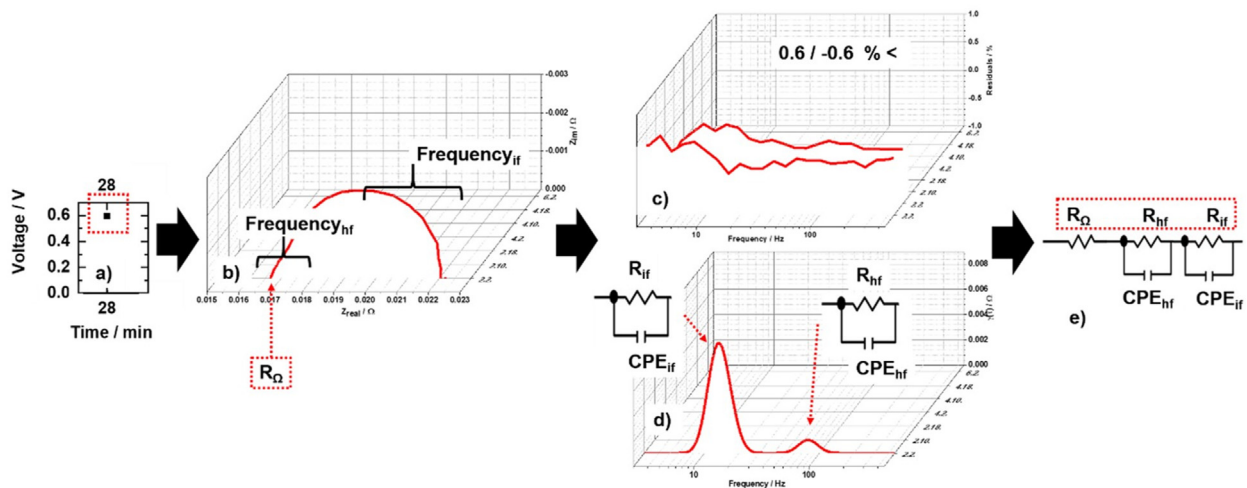


Fig. 2 – Flow chart of data evaluation of a given voltage value (a), the corresponding EIS spectra (b), evaluated K–K validation test (c), DRT analysis (number of processes) (d), corresponding data to be fitted with an equivalent circuit model ECM to obtain resistance values (e).

virtually halted and set to run stable under prolonged regeneration conditions. This helps to recognize the voltage, under which the starvation so far only produced little (reversible) degradation and FC would continue to run in a stable mode. Hence, with our first modelling approach operational strategies may be optimized to prevent FC lifetime reduction.

Experimental setup and data collection

In this study, ANN is trained on empirical data (resistances, voltage, current and time) from a G77 membrane electrode assembly (MEA, Dapozol® Danish Power Systems®) (Yezerka et al. [12,14]). The voltage measurements were performed on a FuelCon AG (Evaluator-C 70316) test station, the current was measured via density distribution device (S⁺⁺ Simulation Services®) and EIS spectra were generated using the potentiostat Ametek Solartron Metrology®. For details on the technical setup see [Supplementary Fig. S1](#) while necessary details are described in the following.

The FCs were cycled in a routine with alternating H₂ starvation and regeneration steps, with gas stoichiometries of $\lambda_A = 1.0$, $\lambda_C = 9.5$ at 0.3 A/cm² (starvation) and $\lambda_A = 1.5$, $\lambda_C = 9.5$ at 0.4 A/cm² (regeneration). The intended oversupply of O₂ avoids any influences from the cathodic side of the FC for clear separation of degradation phenomena on the anode side. The latter is referred to as a 'reference condition'. With an increasing number of starvation steps increasing anode and cathode degradation phenomena occurred. Here, however, electrochemical data from the regeneration steps are used since under reference conditions the FC is expected to operate under stable conditions, and any (irreversible) degradation can only be detected during regeneration by electrochemical means.

Both, output voltage ([Fig. 2a](#)) and current were measured each minute during the operation. The current flow field on the anode side of the FC was placed on the current density distribution device (S⁺⁺ Simulation Services®). The S⁺⁺ unit contains 100 points (intercepts) [14]. The sum of 100 points (current values) is recorded simultaneously to voltage and is typically equal to the applied test station current, being 8.46 A during regeneration ([Fig. S1](#)).

The simultaneously measured EIS data were collected in the frequency range of 10⁻¹ to 10⁴ Hz with an amplitude of 10 mV. The evaluation of EIS data included DRT analysis (Distribution of Relaxation Times) [28], Kramers-Kronig (K–K) validity test [29,30] and EIS data fitting to an electrical circuit model (ECM) [12] as shown in [Fig. 2b–e](#). Hence, these electrochemical data form the base of the inputs to ANN ([Fig. 2f](#)).

The EIS spectra of the 2nd, 10th and 18th minute of each regeneration step were chosen for evaluation. To validate the quality of the obtained EIS spectra the K–K validity test was applied using the freely available MATLAB application Lin-KK Tool. If the relative residuals are within the range of $\pm 1\%$, the impedance data fulfils the Kramers-Kronig relation [5]. In this

work, the residuals of the K–K valid EIS spectra were found within the range $\pm 0.6\%$ ([Figs. S2–S9](#)). Our conservatively chosen test range ensured providing high quality EIS data at a sufficiently high rate. DRT analysis, which serves to evaluate the number of processes during the FC operation was done with freely available MATLAB application DRT tools. Each process is typically attributed to specific frequency ranges, which are common for the underlying electrochemical processes. Among those are ohmic resistivity (R_Ω) at frequencies >100 Hz, charge transfer kinetics of the anode (high frequency (R_{hf}) > 100 Hz) and cathode (intermediate frequency (R_{if}) ~ 10–100 Hz) as well as mass transport (low-frequency range <1 Hz) [31,32]. The resistance R_{hf} is the sum of all processes which typically occur at the anode and R_{if} at the cathode.

Consequently, all spectra are either (1) spectra with a correct EIS response shown by the semi-circle in the Nyquist plot as well as a valid K–K test or (2) spectra with incorrect EIS response and/or an invalid K–K validity test. To evaluate the resistance values the EIS spectra from the group (1) were fitted to an ECM with the ZView® software. In this study, only resistance and no capacitance values (CPE_{hf} and CPE_{if}) are presented because the calculation of these values is much more complex, needs further understanding and is beyond the scope of this contribution.

Process modelling with long short-term memory network

Long Short-Term Memory (LSTM) networks are a type of ANN capable of learning order dependence in sequence prediction problems [33,34]. This behavior is required in composite problem domains like complex chemical processes, such as FC starvation processes. While data fitting methods do not have internal memory and, consequently, they are agnostic with respect to the state of the process, curve fitting methods will not be able to learn and approximate the dynamical model of the FC starvation process.

As any other type of ANN, LSTM network is organized according to [35,36] (see [Fig. 3](#)):

- input layer, which takes the input variables (i.e., voltage, in our case)
- hidden layer, which encodes the complex dynamics (i.e., chemical processes inside FC)
- output layer, which returns the output variables (i.e., R_Ω , R_{hf} and R_{if} resistance, in our case)

Note that the data related to measured currents are not fed into the network since current is a function of voltage and provides redundant information. Data pretreatment or data engineering processes determine which features might be useful in training a model. Such process is commonly known as feature engineering. Feature engineering is the process of

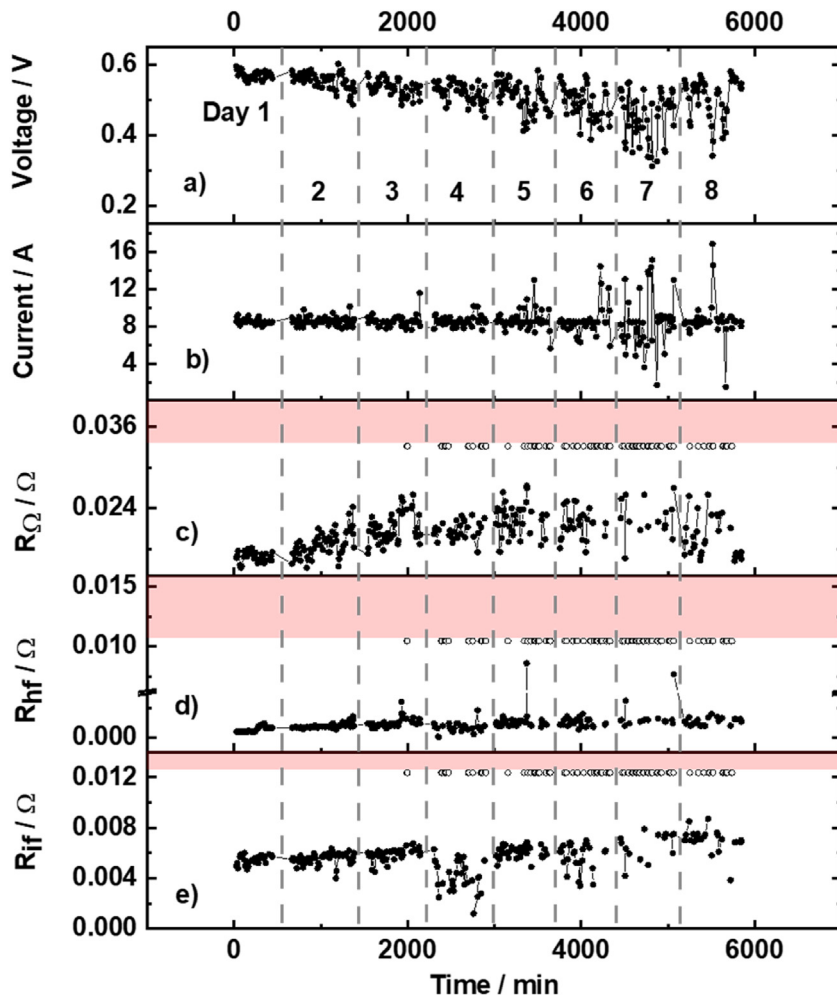


Fig. 4 – Experimental data for a) voltage, b) overall current, c) ohmic resistance R_{Ω} , d) anode resistance R_{hf} , e) cathode resistance R_{if} . Empty circles indicate invalid data according to the Kramers-Kronig validity test, while the pink area shows the region of critical resistances ($R_{K-K \text{ invalid}}$) as defined according to equation (2). Experimental data from Yezerska et al. [12]. (For interpretation of the references to color in this figure legend, the reader is referred to the Web version of this article.)

(except for day 1; Fig. 4c), while R_{hf} increased from 0.0005 Ω to 0.009 Ω (Fig. 4d) and R_{if} increased from 0.005 Ω to 0.009 Ω (Fig. 4e). From day 4, the number of $R_{K-K \text{ invalid}}$ strongly increased, while day 7 included the highest number of $R_{K-K \text{ invalid}}$ data points. Hence, only a few data could be evaluated and used for the ANN data matrix.

In summary, the experimental results showed an overall voltage decrease of ca. 1 mV per regeneration step (Figs. 4a and 5a). However, even more intense voltage decreases were observed during starvation/regeneration routines by other authors (see Introduction). Hence, ANN was trained with the discussed experimental data, and for the study of the behavior of resistances during more intense voltage decreases, three voltage decreases of 3 mV, 5 mV and 10 mV per regeneration step were applied, respectively. Note that, as an initial approach, we only used average voltage decreases without considering fluctuations.

The results show that in scenario 1 (decrease of 3 mV/regeneration step) simulated R_{Ω} , R_{hf} and R_{if} reach $R_{K-K \text{ invalid}}$ at the end of day 2 (Fig. 5b, c, d), which translates to a voltage of 0.51 V short of becoming critical (Fig. 5a). Further, all simulated resistances values rapidly fluctuate between a critical and non-critical state (Fig. 5b, c, d) during the first half of day 3. In scenarios 2 and 3 (decrease of 5 mV and 10 mV) simulated R_{Ω} , R_{hf} and R_{if} reach $R_{K-K \text{ invalid}}$ earlier on day 2 (after ca. 1250 and 1000 min), which translates to voltages of 0.49 V and 0.48 V, respectively. For scenario 2, we note similar rapid fluctuations, however, over a shorter period than in scenario 1, while such rapid fluctuations are absent in scenario 3 (Fig. 5b, c, d).

Hence, from these scenarios, it can be concluded that, according to the voltage decrease, the critically high $R_{K-K \text{ invalid}}$ values are reached at a voltage range between 0.48 and 0.51 V. It is noteworthy that in all scenarios critical $R_{K-K \text{ invalid}}$ values

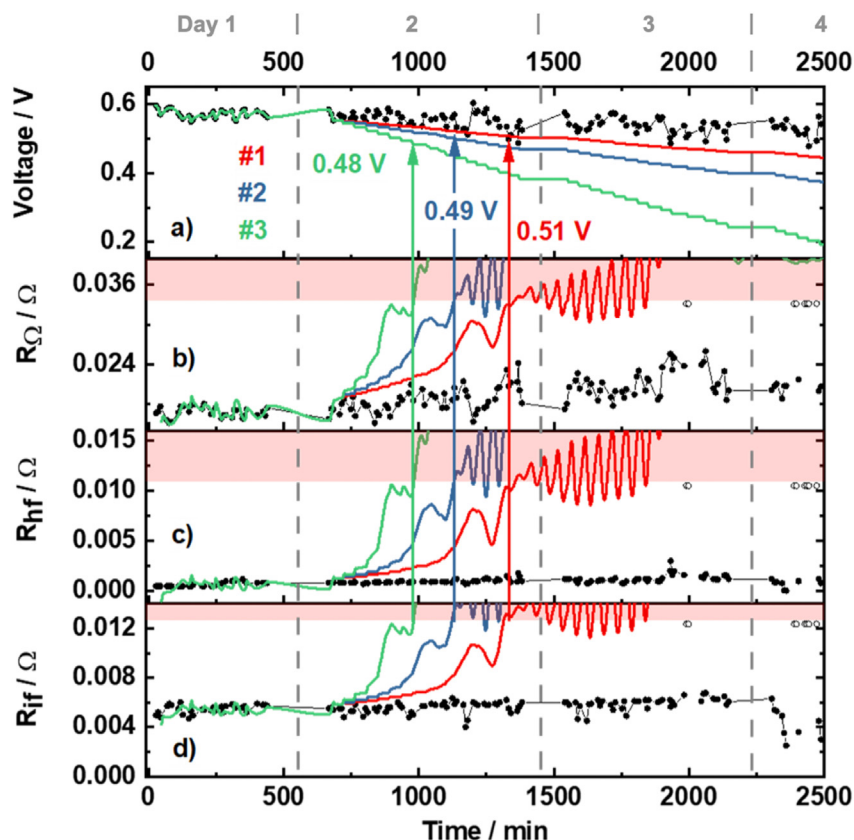


Fig. 5 – Experimental data (black dots) of Yezerska et al.'s [12] FC and simulated data (red, blue and green lines) for three scenarios (#1, 2 and 3) according to applied voltage decreases of 3 mV, 5 mV and 10 mV per regeneration step, a) voltage (see Fig. 4), b) ohmic resistance (R_{Ω}), c) high-frequency resistance (R_{hf}) and d) intermediate frequency (R_{if}) resistance. The pink area shows the region of critical resistances ($R_{K-K \text{ invalid}}$) as defined according to equation (2). (For interpretation of the references to color in this figure legend, the reader is referred to the Web version of this article.)

are reached during day 2. This contrasts with our experimental data, where critical $R_{K-K \text{ invalid}}$ values were obtained much later, essentially on day 4. Hence, any voltage decreases higher than 1 mV per regeneration step is critical and could lead to a premature increase in resistances. We further note that the more intense the voltage decrease is, the less likely the FC switches between a critical and non-critical state. This could mean that more critical (i.e., irreversible) degradation may be reached earlier and more instantaneously, which is a realistic outcome of our simulation.

The aim of our next simulation is to predict whether the FC described by Yezerska et al. [12] would be capable to continue to operate normally (i.e., under regeneration conditions) after a certain degree of starvation. For this, we modelled resistance behaviors at randomly chosen voltage values of 0.48 V, 0.50 V and 0.51 V as shown in scenarios 4, 5, and 6 (Fig. 6).

In scenario 4 (output voltage of 0.48 V), all resistances rapidly increase and reach critical values in the first half of day

4 after ca. 2450 min (Fig. 6). This is roughly in line with the appearance of the first significant number of invalid resistances. We further note an increase in all resistances already on day 3 (after ca. 2000 min), however, this increase remains uncritical. It nevertheless matches the first two invalid resistances on day 3 and, more importantly, the onset of carbon oxidation at the anode which has been inferred from DRT spectra [12]. Hence, our simulation suggests that the FC, which has suffered from starvation and continues to run only at 0.48 V likely remains in a critical, unreliable state from day 4 on.

In scenario 5 (0.50 V), all resistances are elevated and fluctuate between critical and uncritical values on day 3 (Fig. 6). By the end of day 2, all resistances are critically high. The strong fluctuation suggests an insecure behavior of the FC, therefore 0.50 V reflects a limiting scenario.

By contrast, in scenario 6 (0.51 V) although all resistances are elevated as well, they never reach critical values. This

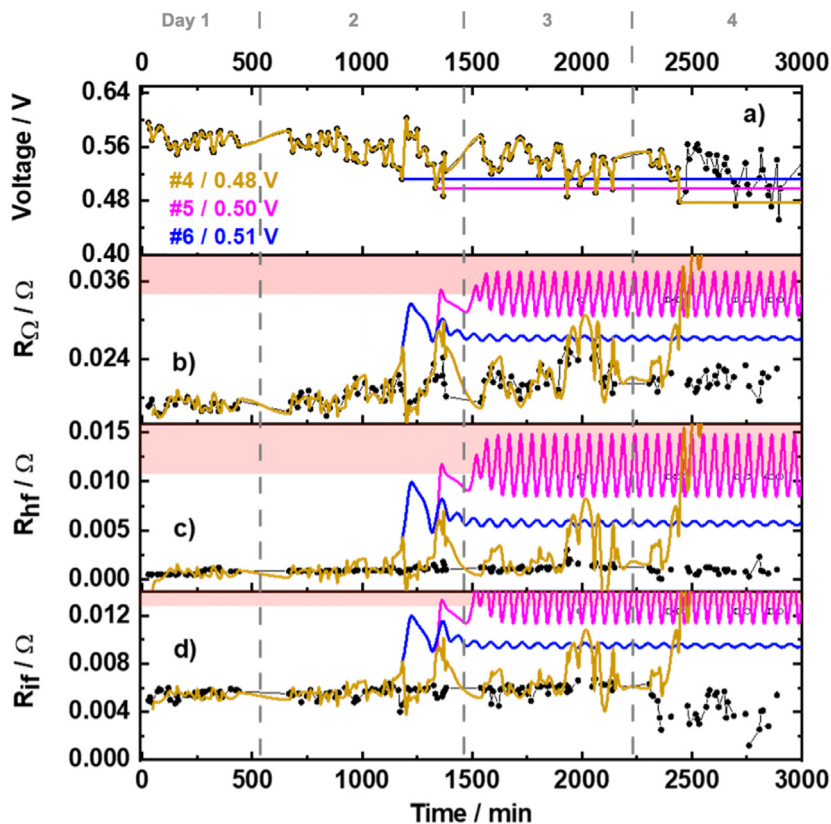


Fig. 6 – Experimental data (black) of Yezerska et al.’s FC (reference) and simulated data for three scenarios under regeneration conditions at constant voltage at 0.48 V (yellow), 0.50 V (magenta) and 0.51 V (blue), a) voltage, b) ohmic resistance (R_{Ω}), c) high frequency resistance (R_{hf}), d) intermediate frequency (R_{if}) resistance. The pink area shows the region of critical resistances (R_{K-K} invalid) as defined according to equation (2). (For interpretation of the references to color in this figure legend, the reader is referred to the Web version of this article.)

suggests that starvation so far only produced little (reversible) degradation and that the FC would continue to run in a stable mode.

Conclusions and Outlook

In this work, a long short-term memory ANN modelling approach for HT-PEM FCs is discussed. The training of the ANN was based on electrochemical data such as resistances calculated from EIS-DRT spectra, voltage, and time. These values were simultaneously measured at high resolution during a long-term fuel (H_2) starvation/regeneration FC cycling routine over 8 days [12]. The calculated resistances were chosen after rigorous quality control determined by a Kramers-Kronig validity test to ensure an accurate data modelling.

In the first ANN application, different voltage decreases, which FCs exhibit during starvation/regeneration routines, were simulated. For this, the voltage decreases of 3 mV, 5 mV and 10 mV per regeneration step were applied in three simulation scenarios. The results showed that (i) critical resistances appeared for output voltages of 0.51 V, 0.49 V and 0.48 V, respectively (compared to the usual reference voltage of 0.6 V), and (ii) as expected, the more intense the voltage

decrease was the sooner these critically high resistances were formed. For example, a voltage decrease of 10 mV would result in severe degradation already on day 2 of cycling.

In the second ANN application, the FC tested by Yezerska et al. [12] was virtually set to continue operating normally, i.e., under regeneration conditions, after certain degrees of starvation. Therefore, the starvation was virtually stopped by keeping the voltage constant at 0.48 V, 0.50 V and 0.51 V. At a voltage of 0.48 V, all simulated resistances rapidly increased and reached critical values on day 4, in line with experimental data. At a voltage of 0.50 V all simulated resistances fluctuated continuously between critical and uncritical values on day 3 suggesting a rather unreliable behaviour of the FC with an unpredictable outcome. However, at a voltage of 0.51 V all simulated resistances were slightly higher but never reached critical values. Hence, our results suggest a secure voltage range between 0.6 V and 0.51 V for a stable FC cycling.

This study showed that an LSTM ANN is a reliable tool for predicting the stress behaviour of a HT-PEM FC. Possible refinements of our modelling approach would be to include fluctuations in the voltage decrease, with ranges according to experimental data. Further, data can be collected from different FCs under starvation and the training approach could be optimized using a k-fold cross-validation.

Declaration of competing interest

The authors declare that they have no known competing financial interests or personal relationships that could have appeared to influence the work reported in this paper.

Acknowledgements

The authors thank the Federal Ministry for Economic Affairs and Energy (Project QUALIFIX, grant ID: 03ET6046A).

Appendix A. Supplementary data

Supplementary data to this article can be found online at <https://doi.org/10.1016/j.ijhydene.2022.06.254>.

REFERENCES

- [1] Rasheed RKA, Liao Q, Caizhi Z, Chan SH. A review on modelling of high temperature proton exchange membrane fuel cells (HT-PEMFCs). *Int J Hydrogen Energy* 2016;42(5):3142–65. <https://doi.org/10.1016/j.ijhydene.2016.10.078>.
- [2] Parthasarathy A, Martin CR. Investigations of the O₂ reduction reaction at the platinum/nafiion interface using a solid state electrochemical cell. *J Electrochem Soc* 1991;138(4):916. <https://doi.org/10.1149/1.2085747>.
- [3] Parthasarathy A, Srinivasan S, Appleby AJ. Temperature dependence of the electrode kinetics of oxygen reduction at the platinum/nafiion® interface—a microelectrode investigation. *J Electrochem Soc* 1992;139(9):2530. <https://doi.org/10.1149/1.2221258>.
- [4] Rosli RE, et al. A review of high-temperature proton exchange membrane fuel cell (HT-PEMFC) system. *Int J Hydrogen Energy* 2017;42(14):9293–314. <https://doi.org/10.1016/j.ijhydene.2016.06.211>.
- [5] Weiß A, Schindler S, Galbiati S, Danzer MA, Zeis R. Distribution of relaxation times analysis of high-temperature PEM fuel cell impedance spectra. *Electrochim Acta* 2017;230:391–8. <https://doi.org/10.1016/j.electacta.2017.02.011>.
- [6] Sahlin SL, Araya SS, Andreasen SJ, Kær SK. Electrochemical impedance spectroscopy (EIS) characterization of reformat-operated high temperature PEM fuel cell stack. *Int. J. Power Energy Res.* 2017;1(1). <https://doi.org/10.22606/ijper.2017.11003>.
- [7] Ji M, Wei Z. A review of water management in polymer electrolyte membrane fuel cells. *Energies* 2009;2(4):1057–106. <https://doi.org/10.3390/en20401057>.
- [8] Zhou F, Andreasen SJ, Kær SK, Yu D. Analysis of accelerated degradation of a HT-PEM fuel cell caused by cell reversal in fuel starvation condition. *Int J Hydrogen Energy* 2015;40(6):2833–9. <https://doi.org/10.1016/j.ijhydene.2014.12.082>.
- [9] Araya SS, et al. A comprehensive review of PBI-based high temperature PEM fuel cells. *Int J Hydrogen Energy* 2016;41(46):21310–44. <https://doi.org/10.1016/j.ijhydene.2016.09.024>.
- [10] Arama FZ, Mammarr K, Laribi S, Necaibia A, Ghaitaoui T. Implementation of sensor based on neural networks technique to predict the PEM fuel cell hydration state. *J Energy Storage* 2020;27:101051. <https://doi.org/10.1016/j.est.2019.101051>.
- [11] J. T. Pukrushpan, A. G. Stefanopoulou, H. Peng, and A. Arbor, “Control of Fuel Cell Breathing: Initial Results on the Oxygen Starvation Problem,” *Fuel Cell*, vol. 1, no. 734, pp. 1–25, doi: <https://doi.org/10.1109/MCS.2004.1275430>.
- [12] Yezerska K, et al. Analysis of the regeneration behavior of high temperature polymer electrolyte membrane fuel cells after hydrogen starvation. *J Power Sources* 2020;449:227562. <https://doi.org/10.1016/j.jpowsour.2019.227562>.
- [13] Danzer MA. Generalized distribution of relaxation times analysis for the characterization of impedance spectra. *Batteries* 2019;5(3):1–16. <https://doi.org/10.3390/batteries5030053>.
- [14] Yezerska K, et al. Characterization methodology for anode starvation in HT-PEM fuel cells. *Int J Hydrogen Energy* 2019;44(33):18330–9. <https://doi.org/10.1016/j.ijhydene.2019.05.114>.
- [15] Ramón-Fernández A, Salar-García MJ, Fernández DR, Greenman J, Ieropoulos IA. Evaluation of artificial neural network algorithms for predicting the effect of the urine flow rate on the power performance of microbial fuel cells. *Energy* 2020;213. <https://doi.org/10.1016/j.energy.2020.118806>.
- [16] Porwal U, Shi Z, Setlur S. Chapter 18 - Machine learning in handwritten Arabic text recognition, 31; 2013. <https://doi.org/10.1016/B978-0-444-53859-8.00018-7>.
- [17] Kröse B, van der Smagt P. Introduction to neural networks. *Int J Join Mater* 1994;6(1):4–6. <https://doi.org/10.5860/choice.35-5700>.
- [18] Roh Y, Heo G, Wang SE. A survey on data collection for machine learning: a big data - AI integration perspective. *IEEE Trans Knowl Data Eng* 2021;33(4):1328–47. <https://doi.org/10.1109/TKDE.2019.2946162> [Online].
- [19] Conrad E, Misener S, Feldman J [Chapter 9] - Domain 8: Software Development Security (Understanding, Applying, and Enforcing Software Security), <https://doi.org/10.1016/B978-0-12-802437-9.00009-6>; 2016.
- [20] Shao M, Zhu XJ, Cao HF, Shen HF. An artificial neural network ensemble method for fault diagnosis of proton exchange membrane fuel cell system. *Energy* 2014;67:268–75. <https://doi.org/10.1016/j.energy.2014.01.079>.
- [21] Mohammadi A, Guilbert D, Gaillard A, Bouquain D, Khaburi D, Djerdir A. Faults diagnosis between PEM fuel cell and DC/DC converter using neural networks for automotive applications. *IECON Proc. (Industrial Electron. Conf. 2013:8186*. <https://doi.org/10.1109/IECON.2013.6700503>. –8191.
- [22] T. Kavzoglu, “An investigation of the design and use of feed-forward artificial neural networks in the classification of remotely sensed images”. PhD thesis 2001, Nottingham University, United Kingdom. <http://hdl.handle.net/10068/625504>
- [23] Panchal G, Ganatra A, Kosta YP, Panchal D. Behaviour analysis of multilayer perceptrons with multiple hidden neurons and hidden layers. *Int J Comput Theory Eng* 2011;3(2):332–7. <https://doi.org/10.7763/IJCTE.2011.V3.328>.
- [24] Akkaya AV. Neural Network approach for performance prediction of a SOLID oxide fuel cell. *Technology* 2009;12(3):211–6.
- [25] Laribi S, Mammarr K, Hamouda M, Sahli Y. Impedance model for diagnosis of water management in fuel cells using artificial neural networks methodology. *Int J Hydrogen Energy* 2016;41(38):17093–101. <https://doi.org/10.1016/j.ijhydene.2016.07.099>.
- [26] Xie R, Ma R, Pu S, Xu L, Zhao D, Huangfu Y. Prognostic for fuel cell based on particle filter and recurrent neural network fusion structure. *Energy AI* 2020;2:100017. <https://doi.org/10.1016/j.egyai.2020.100017>.

- [27] Gu X, Hou Z, Cai J. Data-based flooding fault diagnosis of proton exchange membrane fuel cell systems using LSTM networks. *Energy AI*; 2021, 100056. <https://doi.org/10.1016/j.egyai.2021.100056>.
- [28] Wan TH, Saccoccio M, Chen C, Ciucci F. Influence of the discretization methods on the distribution of relaxation times deconvolution : implementing radial basis functions with DRTtools. *Electrochim Acta* 2015;184(October):483–99. <https://doi.org/10.1016/j.electacta.2015.09.097>.
- [29] Boukamp BA. A linear kronig - Kramers transform test for immittance data validation. *J Electrochem Soc* 1995;142(6):1885–94.
- [30] Schönleber M, Klotz D, Ivers-Tiffée E. A method for improving the robustness of linear kramers-kronig validity tests. *Electrochim Acta* 2014;131:20–7. <https://doi.org/10.1016/j.electacta.2014.01.034>.
- [31] Schindler S, Weiß A, Galbiati S, Mack F, Danzer MA, Zeis R. Identification of polarization losses in high temperature PEM fuel cells by distribution of relaxation times analysis. *ECS Trans* 2016;75(14):45–53. <https://doi.org/10.1149/07514.0045ecst>.
- [32] Mack F, Laukenmann R, Galbiati S, Kerres JA, Zeis R. Electrochemical impedance spectroscopy as a diagnostic tool for high-temperature PEM FuelCells. *ECS Trans* 2015;69(17):1075–87. <https://doi.org/10.1149/06917.1075ecst>.
- [33] Wang C, Li Z, Outbib R, Dou M, Zhao D. A novel long short-term memory networks-based data-driven prognostic strategy for proton exchange membrane fuel cells. *Int J Hydrogen Energy* 2022;47(18):10395–408. <https://doi.org/10.1016/j.ijhydene.2022.01.121>.
- [34] Liu J, Li Q, Chen W, Yan Y, Qiu Y, Cao T. Remaining useful life prediction of PEMFC based on long short-term memory recurrent neural networks. *Int J Hydrogen Energy* 2019;44(11):5470–80. <https://doi.org/10.1016/j.ijhydene.2018.10.042>.
- [35] Çalık A, Yıldırım S, Tosun E. Estimation of crack propagation in polymer electrolyte membrane fuel cell under vibration conditions. *Int J Hydrogen Energy* 2017;42(36):23347–51. <https://doi.org/10.1016/j.ijhydene.2017.02.119>.
- [36] Seyhan M, Akansu YE, Murat M, Korkmaz Y, Akansu SO. Performance prediction of PEM fuel cell with wavy serpentine flow channel by using artificial neural network. *Int J Hydrogen Energy* 2017;42(40):25619–29. <https://doi.org/10.1016/j.ijhydene.2017.04.001>.